Polymer Chemistry

Spatiotemporal Control over the Host-Guest Characteristics of a Stimulus-Triggerable Trifunctional Polymer Assembly

Journal:	*Polymer Chemistry*
Manuscript ID	PY-ART-12-2018-001788.R1
Article Type:	Paper
Date Submitted by the Author:	25-Jan-2019
Complete List of Authors:	Khomein, Piyachai; University of Massachusetts, Department of Chemistry Dutta, Kingshuk; University of Massachusetts, Department of Chemistry Gnanasekaran, Karthikeyan; Northwestern University Gianneschi, Nathan; Northwestern University, Chemistry; University of California, San Diego, Chemistry and Biochemistry Thayumanavan, Sankaran; University of Massachusetts, Department of Chemistry

Polymer Chemistry

Paper

Spatiotemporal Control over the Host-Guest Characteristics of a Stimulus-Triggerable Trifunctional Polymer Assembly

Received 00th January 20xx,
Accepted 00th January 20xx

DOI: 10.1039/x0xx00000x

www.rsc.org/

Piyachai Khomein,[a] Kingshuk Dutta,[a] Karthikeyan Gnanasekaran,[b] Nathan C. Gianneschi,[b] and S. Thayumanavan*[a]

The positional effect of stimuli-responsive units in tri-component copolymer vesicles is studied to explore variations in the host-guest properties of the assembly. We study this by placing pH-responsive diisopropylaminoethyl moieties in three distinct locations of a block copolymer assembly. In two of the three variations, these functionalities were randomly distributed in the hydrophobic or the hydrophilic domains of an amphiphilic diblock copolymer. In a third variation, this responsive functionality was incorporated as the middle block in a triblock copolymer. The results reveal that the solvent exposure of the responsive units holds the key for controlling the rate of molecular release from these polymer vesicles. The study also shows that equilibrium changes in the morphology of an assembly are not good indicators of the responsive host-guest properties of a polymer assembly.

Introduction

Amphiphilic block copolymers that can self-assemble in water have gained substantial interest in both academia and industry.[1-3] The interest stems from the ability to predictably tune structures to generate various morphologies starting from simple spherical micelles,[4-5] rod-shaped particles[6-8] and vesicles[9-12] to complex morphologies such as Janus particles.[13-15] This feature opens up many possible applications, including, but not limited to biomedical delivery,[16-18] sensors,[19-21] electronic devices[22-24] and catalysts.[25-27] In general, self-assembly of these polymers is driven by three factors related to the free energy of the system: the degree of stretching of the polymer chain, the curvature and interfacial tension energy.[28] Therefore, the morphology of the self-assembly can be manipulated by polymer composition, concentration, and/or the nature of solvents used for the assembly process.

Among the various morphologies studied, polymeric vesicles or polymersomes are particularly interesting from the perspective of host-guest characteristics, because these assemblies can simultaneously bind to both hydrophilic and hydrophobic guest molecules within their lumen and the polymer-based membrane space respectively.[9-12] The host character of these assemblies can then be exploited for many applications, if these assemblies can be triggered to release the sequestered guests in response to a specific stimulus.[29-36] Among the stimuli studied, pH has gained particular attention, inspired by the significant variations in the acidity of various sub-cellular compartments and pathological extracellular microenvironments in biological systems.

The idea of incorporating pH-responsive functional groups in copolymer assemblies and utilizing the pH-induced changes in the hydrophilic-lipophilic balance of the polymer to alter the assembly characteristics is indeed quite well studied.[37-41] In these studies that involve block copolymer assemblies, the pH-responsive unit is invariably placed in the hydrophobic block.[37,38] This is intuitively understandable, because a change in the hydrophilicity of this block is likely to have the greatest impact on the host-guest fidelity of the assembly. We were however intrigued by the seemingly different requirement in the first step of this process, which needs protons to diffuse into the hydrophobic part of the polymer membrane. To assess the relative effects of these two counter-acting effects, we envisaged the possibility of placing the responsive moieties at different locations of a tri-component block copolymer assembly and assess the effect of pH upon its host-guest characteristics (**Scheme 1**). In this manuscript, we disclose our

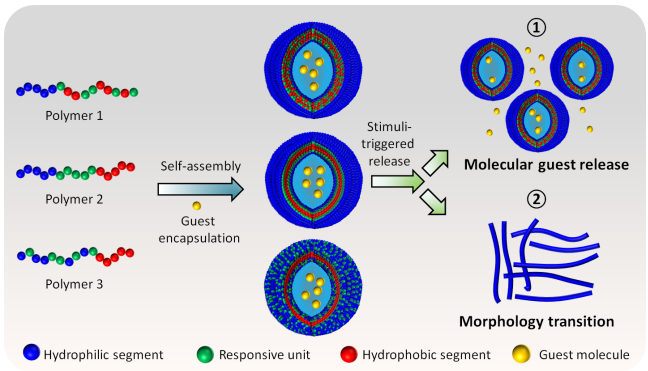

Scheme 1. Schematic diagram of designed polymeric vesicle assemblies.

[a] Department of Chemistry, University of Massachusetts, Amherst, MA 01003, United States.
[b] Department of Chemistry, Northwestern University, Evanston, Illinois 60208, United States

†Electronic Supplementary Information (ESI) available. See DOI: 10.1039/x0xx00000x

findings on the relative kinetics of pH-induced molecular release from each of these assemblies.

Results and Discussion

Design, synthesis and characterizations of polymers

The structure of our polymer assemblies is based on a diblock copolymer type assembly, containing a hydrophilic and hydrophobic block to facilitate vesicular assemblies in aqueous media. The hydrophilic block is based on poly(poly(ethylene glycol) methyl ether acrylate) (PPEGA), while the hydrophobic block is based on polybutyl acrylate (PBuA). The critical third component of the polymer is based on the 2-(diisopropylamino)ethyl acrylate (DIPA) monomer. This pH-responsive component was distributed within the block copolymer in three different ways: (*i*) incorporated randomly in the hydrophobic block along with PBuA; (*ii*) inserted as the middle block between the PBuA and PPEGA blocks; (*iii*) incorporated randomly in the hydrophilic block along with PPEGA. Thus, the targeted polymers **1-3** with these characteristics are shown in **Scheme 2**.

The polymers **1-3** were synthesized using reversible addition-fragmentation chain-transfer (RAFT) polymerization. Synthesis of polymer **1** started with the polymerization of poly(ethylene glycol)methylether acrylate (PEGA) monomer using a RAFT initiator to obtain the PPEGA macroinitiator, as shown in Scheme 3. This macroinitiator was then used for the random copolymerization of DIPA and buthylacrylate (BuA) monomers to obtain polymer **1** with a MW of 28.0 kg/mol and a Đ of 1.45. Similarly, polymer **2** was synthesized by sequentially polymerizing the DIPA monomer, followed by the BuA monomer, using the PPEGA macroinitiator to afford the triblock copolymer with a MW of 30.5 kg/mol and a Đ of 1.45. On the other hand, synthesis of polymer **3** was achieved by carrying out a RAFT random copolymerization of PEGA and DIPA monomers. This polymer was then used as the macroinitiator to polymerize the BuA monomer to obtain polymer **3** with a MW of 38.0 kg/mol and a Đ of 1.55.

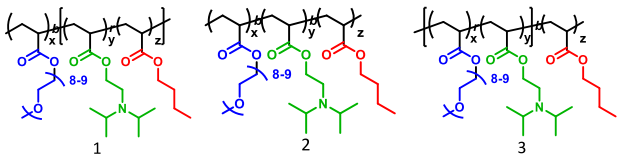

Scheme 2. The structures of tri-component polymers **1 – 3.**

Solvent addition method was used to form the targeted assemblies in water for polymers **1**-**3**. Assembly sizes for all three polymers were found to be in the range of 70-90 nm, as characterized by dynamic light scattering (DLS) (**Figure 1a**). Next, we interrogated the assemblies for their morphology. Cryogenic transmission electron microscopy (cryo-TEM) analysis of the assemblies showed that all three polymers form hollow spherical assemblies, indicative of the targeted vesicular structures in solution (**Figure 1c**). The vesicular morphology was further confirmed by determining the ratio between radius of gyration (R_g) and hydrodynamic radius (R_h). This ratio is referred to the shape factor in which 0.77 corresponds to solid sphere,

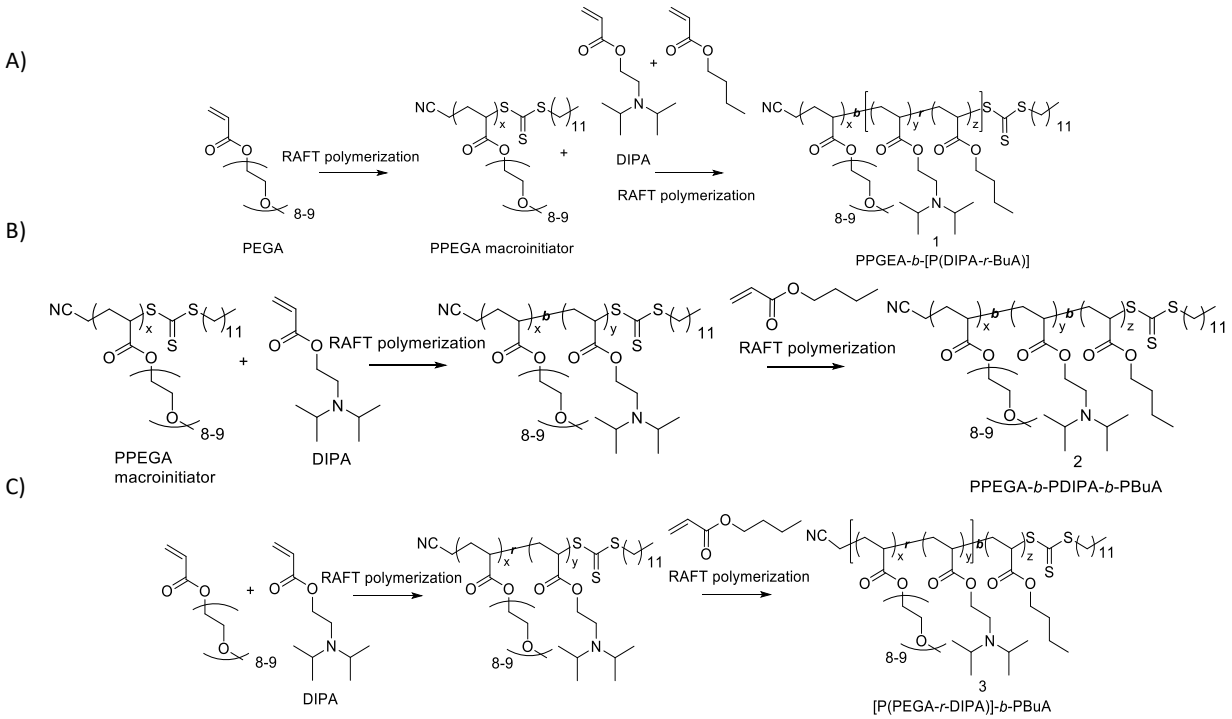

Scheme 3. Synthesis of polymer **1** (A), **2** (B), and, **3** (C).

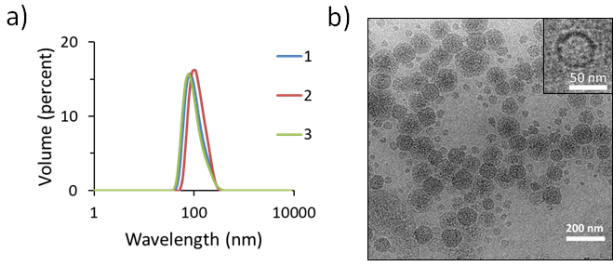

Figure 1. Size distributions (a) of the polymer assembly **1**-**3** in water at concentration of 1 mg/mL and Cryo-TEM image of polymer assembly **3** (b).

1.00 indicates hollow sphere and 1.54 dictates random-coil morphology of the polymer[42]. Static light scattering (SLS) was used to evaluate R_g values, while R_h was determined from DLS measurements. Indeed, the polymer assemblies of **1**-**3** have the shape factor (R_g/R_h) of 1.05, 1.04 and 0.97 respectively, supporting the vesicular morphology (see ESI† for details).

Vesicular assemblies are capable of encapsulating both hydrophilic and hydrophobic guest molecules. To explore this feature, calcein was used as the hydrophilic fluorescent guest molecule that gets encapsulated within the lumen of the assembly. This is a good probe for evaluating encapsulation, because of its self-quenching characteristics. When the molecule is present inside the assembly, the local concentration of the dye is high in the lumen of the vesicle, even if the overall solution concentration is low. In this case, we first encapsulated calcein within the assemblies obtained from **1-3**. The absorbances of these solutions were matched with an aqueous solution of calcein. Comparison of the fluorescence spectra from these solutions showed that the calcein emission from the polymeric assemblies were substantially lower (**Figure 2**), although the global concentration of all the solutions are similar. This suggests that calcein is indeed encapsulated within the polymeric assemblies. Similarly, the possibility of encapsulating hydrophobic molecules was studied using Nile red as the guest. Note that this dye molecule is not soluble in aqueous phase by itself. However, in the presence of the polymer assemblies, significant amount of Nile red was solubilized in the aqueous phase, suggesting that the polymeric assemblies can act as a host for these hydrophobic molecules also (see ESI† for details).

Kinetics of guest release

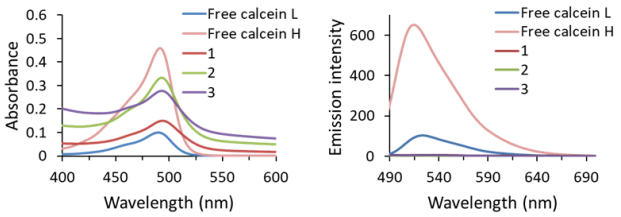

Figure 2. Absorption (a) and emission spectra (b) of free calcein at low (L) and high (H) concentration and encapsulated calcein in polymer assemblies.

Next, the effect of varying the placement of the pH-responsive groups in the polymer backbone was investigated with respect to the host-guest characteristics of the assembly. It is reasonable to hypothesize that the random incorporation of the responsive groups in the hydrophobic part should have the highest impact in molecular release, as hydrophobic driving force is the primary influence on the stability of such polymer assemblies. At acidic pH, DIPA units in the polymer backbone would be in their protonated form, thus switching from a hydrophobic amine to a more hydrophilic ammonium salt. We surmised that the resultant change in the hydrophobicity of the membrane could result in rapid release of guest molecules. However, the accessibility of the trigger molecules (proton diffusion) could be hindered due to hydrophobic butylacrylate moieties in the assembly creating a barrier for molecular release response. On the other hand, the random incorporation of the responsive groups in hydrophilic part would allow ready access to the trigger molecules. However, this is expected to have minimal impact on the vesicle membrane stability, because the pH-induced change in the hydrophilic-lipophilic balance largely occurs in the already solvent-exposed portion of the assembly.

Accordingly, we monitored the release of calcein at lower pH, *i.e.* pH 4, and compared it with that at ambient pH, *i.e.* pH 7. Since the calcein fluorescence was quenched when they are encapsulated inside the vesicle, a recovery of their fluorescence signal will be observed if the container property of the polymeric assembly is compromised. Interestingly indeed, the calcein fluorescence was found to increase, when the pH of the solution containing the polymeric assembly was exposed to the acidic pH 4, implying that calcein is being released from the vesicles (**Figure 3 a-c**). In the control solutions at pH 7, there was no discernible change in the calcein fluorescence within the same time frame (**Figure 3 d-f**).

To more quantitatively analyze the molecular release from these assemblies, we monitored the rate of molecular release through the fluorescence recovery measurements. Since the extent of fluorescence recovery is directly proportional to molecular release, we used this as the semi-quantitative measure. However, note that there is no known linear relationship between the fluorescence recovery from quenching and the number of molecules released from the assembly. Therefore, while the fluorescence recovery provided a semi-quantitative measure of how the fidelity of the polymeric assembly is compromised by the change in pH, we could not assign a clear kinetic order for this process. Considering this, we became primarily interested in comparing the relative rates of molecular release from these three assemblies, which was obtained from the slope of fluorescence increase in the linear regime of the plots at short time scales (**Figure 4**).

Comparison of these slopes for the polymeric assemblies **1-3** offered an interesting trend. The linear slope for the assembly from **1** was found to be ~0.012, while those from **2** and **3** were measured to be ~0.030 and ~0.059 respectively. These results were counter to the more conventional expectation that the highest impact would be in the hydrophobic block of the copolymer assembly. Instead here, the pH-induced change in the host characteristics of the assembly seems to be the greatest when the stimulus-responsive functional group is randomly distributed in the hydrophilic block. The kinetics of molecular release seem to be ~5 times or 6 faster, when the responsive moieties are in the hydrophilic PPEGA block, compared to when these functionalities are distributed in the hydrophobic PBuA block. When the responsive units are distributed at the interface between the two blocks, the kinetics seem to fall in between the two rates.

We could reason that the rate of guest release can be correlated to accessibility of protons for the responsive units in polymer structure. Since the assembly **3** possesses the most exposed responsive groups where they were oriented randomly in hydrophilic part, it exhibits fastest molecular release. On the other hand, the responsive groups were buried inside the hydrophobic membrane in assembly **1**, thus exhibiting the slowest calcein release. Since the placement of responsive moieties in **2** represents a scenario that is in between those represented by **1** and **3**, the intermediate release rate from assembly **2** seems to be consistent with this assertion. However, we were concerned that it is also possible that the trend in release rate might be specific to this particular copolymer structure. This concern stems from the fact that PPEGA segment of this copolymer contains rather long oligoethyleneglycol moieties with 8-9 repeating units, thus possessing the features of a short polymer brush. Therefore, it is possible that it is this brush-like hydrophilic block that offers significant barrier to accessing the interiors of the polymer membrane. To distinguish these possibilities, we designed a structurally similar set of polymers, but without the brush-like characteristics.

Synthesis and characterizations of hydroxyethylacrylate polymers

To test the hypothesis, we designed and synthesized polymers **4**-**6**, where the hydrophilic component of the polymer is changed from PPEGA to poly(2-hydroxyethyl acrylate) (PHEA). Syntheses of polymers **4** and **5** were achieved using a route similar to that outlined for polymers **1** and **2** respectively. The details of the synthetic procedures for these polymers are outlined in the Experimental Section. Briefly, polymer **4** was obtained with a MW of 20,000 g/mol and a Đ of 1.87, while polymer **5** was achieved with a MW of 38.0 kg/mol and a Đ of 1.62. In the syntheses of these two polymers, PEGA monomer was simply replaced with HEA monomer in the synthetic strategy. However, this approach was not successful in the synthesis of polymer **6**, where the hydroxyl moiety of the HEA monomer had to be protected with a *tert*-butyldimethylsilyl group as shown in **Scheme 4**. When we simply followed the procedure, similar to that used for obtaining **3**, we observed an insoluble polymer that is presumably crosslinked. The reason for this difficulty is not understood at this time. Nonetheless, this was overcome by using a protected monomer, which was then deprotected in a post-polymerization step, as shown in **Scheme 4,** to give polymer **6** with a MW of 24.0 kg/mol and a Đ of 1.25.

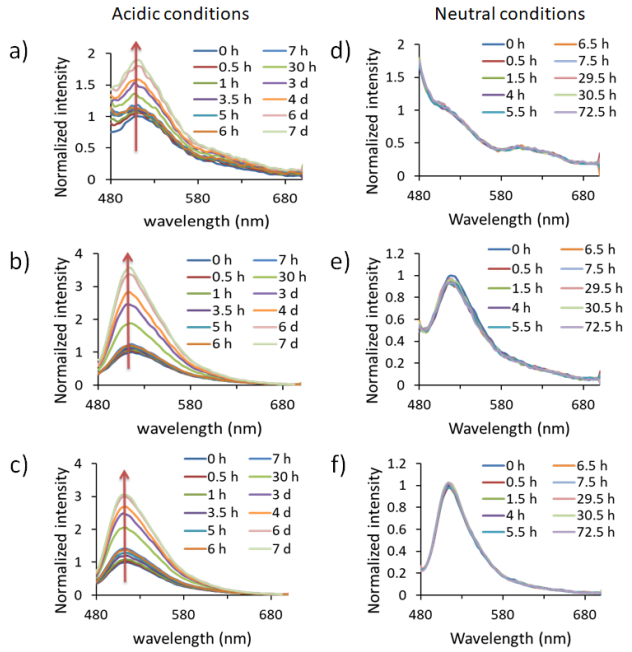

Figure 3. Normalized fluorescence intensity recovery of calcein in acidic condition (a-c) and neutral condition (d-f) for polymer assemblies **1** (a, d), **2** (b, e), and **3** (c, f).

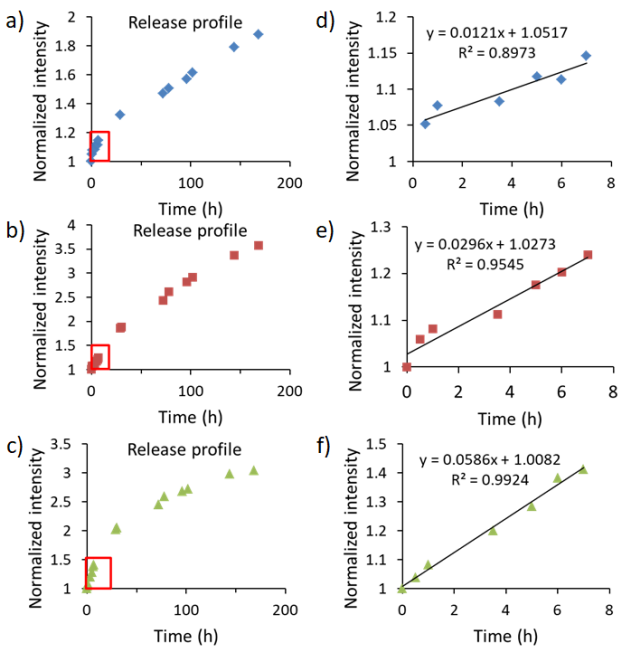

Figure 4. Release profile of calcein and linear regression fit for polymer assemblies **1**(a, d), **2** (b, e) and **3**(c, f), respectively.

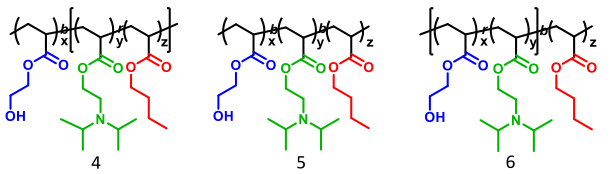

4 5 6

PHEA-*b*-[P(DIPA-*r*-BuA)]) (PHEA-*b*-PDIPA-*b*-PBuA) ([P(HEA-*r*-DIPA)]-*b*-PBuA)
x = 30, y = 112, z = 75 x =30, y = 113, z =199 x = 28, y = 68, z = 106
MW = 20,000 Đ = 1.87 MW = 38,000 Đ = 1.62 MW = 24,000 Đ = 1.25

Scheme 4. The structures of tri-component polymers **4** – **6.**

Here too, solvent addition method was used to form the assemblies for polymers **4**-**6**. Interestingly, the assembly sizes for these polymers were found to be ~10 times larger than those from polymers **1**-**3**, as measured using DLS. The larger size of the assemblies offered the opportunity to analyze these assemblies using optical microscopy. Indeed, these images further confirmed the assembly sizes to be in the range of 1-5 µm (**Figure 5c**). To assess whether the reason for these self-assembled structures, resulting in differences in size, could be due to factors other than the variation in the structure of the hydrophilic moiety, we studied the effect of the solvent used for preparing these assemblies. Note that all copolymers **1-6** have similar hydrophilic content (7-11%wt). Similarly, the procedures for preparing these assemblies were also identical. Thus, the possible factors could be the nature of solvents and/or the difference in the polymer structure of the hydrophilic segment. Acetone and DMF were used as solvents to prepare the assemblies for polymers **1**-**3** and **4**-**6**, respectively.

Although both solvents were attempted for all six polymers, the HEA polymers **4-6** could not be easily dissolved in acetone. Therefore, the assemblies were achieved successfully, only in DMF. However, our detailed studies with polymers **1-3** were initially carried out with assemblies, which used acetone as the co-solvent in the self-assembly media. To investigate whether the assembly size variations can be achieved with variations in the solvent, the polymer assemblies of **1**-**3** were prepared in DMF. If the nature of solvent is the reason behind the difference in sizes between the two sets of polymers, bigger assemblies should be observed in case of DMF. However, the aggregate sizes of the polymer assembly of **1**-**3** were still in the range of 70-90 nm. Therefore, the difference in the assembly sizes was attributed to the nature of the hydrophilic group. Since PHEA contains shorter hydroxyethyl moieties, compared to the bulkier structure of PPEGA, it is possible that there is an increase the curvature of the latter assemblies, which in turn results in a decrease in the size of the vesicles.

As anticipated, assemblies **4**-**6** were also found to encapsulate both calcein and Nile red (**Figure S3** in ESI†). We

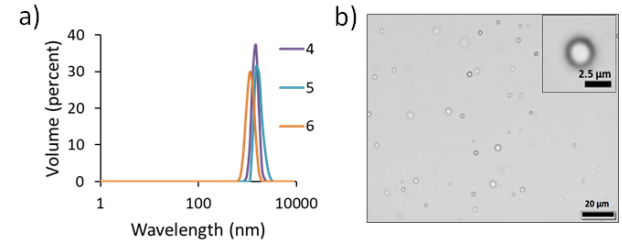

Figure 5. Size distributions (a) of the polymer assembly **4**-**6** in water at concentration of 1 mg/mL; Optical microscope image of the assembly **4** in water (c).

further confirmed the dye encapsulation from these polymer assemblies with confocal laser scanning microscopy (CLSM, **Figure 6**). The images clearly demonstrated the vesicle-type morphology in which Nile red (red fluorescence channel) occupied the hydrophobic part of the membranes and calcein (green fluorescence channel) stayed in the water pool inside the vesicles. The co-localization of Nile red with calcein, combined with the z-stack images (**Figure S4** in ESI†), further confirmed the location of hydrophobic and hydrophilic dyes. Since acetone was used as a solvent for Nile red, the apparent partial penetration of the hydrophobic dye from the membrane to the hydrophilic core was attributed to the solubility of acetone in water that affords some co-localization of the red and green dyes in the vesicles.

Kinetic of guest release from the hydroxyethylacrylate polymer

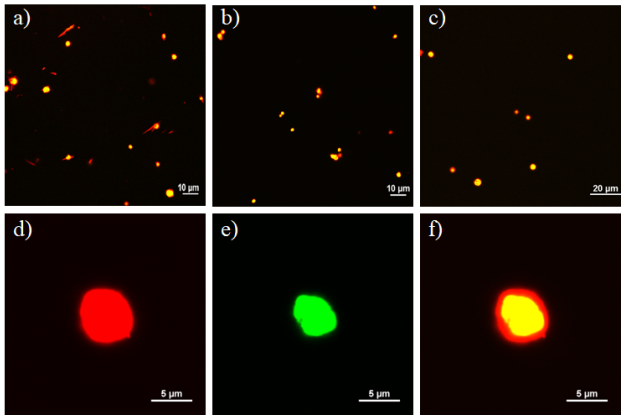

Figure 6. Confocal images of polymer assembly **4** (a), **5** (b) and **6** (c); A single vesicle-type particle originated from polymer assembly **4**: red channel (d), green channel (e) and merged channel (f).

assemblies

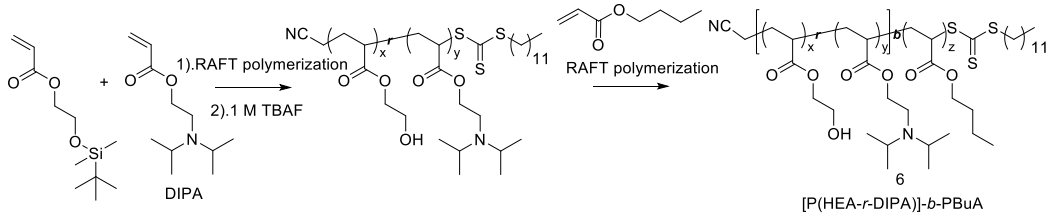

Scheme 5. Synthesis of polymer **6**.

If the brush-like characteristic of PPEGA slows the pH-induced rate of release of the encapsulated guest molecules, the less bulkier PHEA should allow protons to more readily access the responsive units in the assemblies obtained polymers **4**-**6**. The calcein release profiles and linear regression fit for the earlier time scale are shown in **Figure 7**. Assembly **6**, with the responsive DIPA units randomly positioned in the hydrophilic part of the block copolymer, exhibited the fastest release among the three assemblies with a slope of 0.043. The rate of release from assembly **5** was found to be faster than that from **4**, but slower than that from **6**. The overall trend in relative guest release rates from each of these PHEA assemblies is similar to that observed from PPEGA assemblies **1-3**. These results further confirm that the location of the responsive moieties has significant implications in the guest release rate from these pH-responsive supramolecular assemblies. Additionally, the difference in release rate of guest molecules between the fastest (assembly **6**) and the slowest (assembly **4**) assembly was found to be smaller (2x), compared to the difference between the corresponding PPEGA assemblies **1** and **3** (5x). This could be attributed to the difference in accessibility to the responsive units, because of the bulkier PEGA moieties. Alternatively, this could also simply be a manifestation of the difference in size of the assemblies, where the smaller assembly with the higher surface-to-volume ratio exhibits higher release rates.

In addition to calcein release from the lumen of the vesicles, we also investigated the release of the hydrophobic Nile red in response to pH change from neutral to acidic conditions using absorption spectroscopy. Since the solubility of Nile red in water is very poor, it would precipitate upon release from the assemblies and a decrease in UV-Vis absorption would be observed. However, the release of Nile red was not found to be significant after the pH-based triggering of all these assemblies. This could be due to the possibility that the product assemblies in response to the pH change is capable of providing a reservoir for the hydrophobic molecules, as the bulk aqueous environment is not the preferred environment for these molecules (**Figure S7** and **S8** in ESI†).

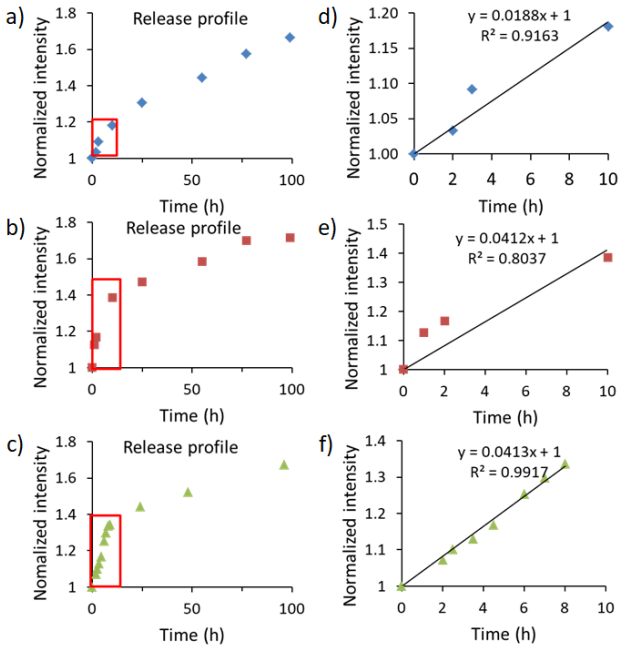

Figure 7. Release profile of calcein and linear regression fit for polymer assemblies **4** (a, d), **5** (b, e) and **6** (c, f), respectively.

To further assess this possibility, the morphological transitions for the assemblies **4**-**6** were analyzed at pH 4 after 2 days using CLSM (**Figure 8**). Interestingly, the morphology of assembly **4** completely changed from vesicle to a needle like structure (**Figures 8 and 9**). In polymer assembly 4, the responsive units were randomly placed in the hydrophobic membrane. Thus, it is expected to have significant impact on morphological transformation, because of the hydrophobic to hydrophilic modification of the responsive units under acidic conditions. We hypothesize that the sphere-to-rod transition is governed by the changes in molecular packing. Moreover, the large extent of randomness in the hydrophobic-responsive segment of polymer 4 backbone presumably makes the system more manipulatable by the pH change. This result is indeed consistent with the interest in incorporating responsive units in the hydrophobic block of a diblock copolymer, as most of these studies have focused on evaluating the morphological changes in the assembly[35, 40, 43-45]. On the other hand, the morphology of the assemblies **5**-**6** remained as vesicle with comparable red fluorescence intensity at vesicle membrane, while the green fluorescence was significantly lesser inside the vesicle water pool. The size also became smaller, compared to the vesicles

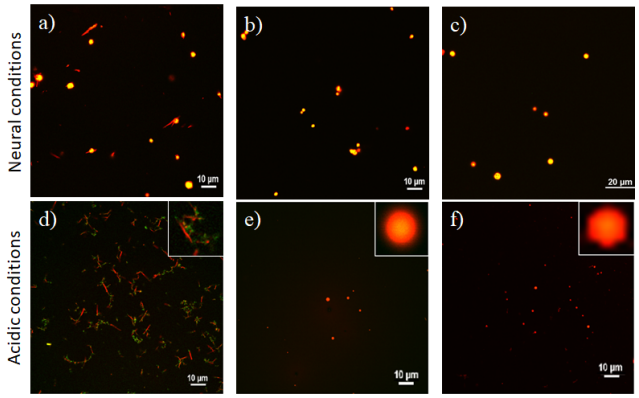

Figure 8. The confocal fluorescence microscopy images of the assemblies **4** (a, d), **5** (b, e) and **6** (c, f) at neutral pH (top) and after 2 days at pH 4 (bottom).

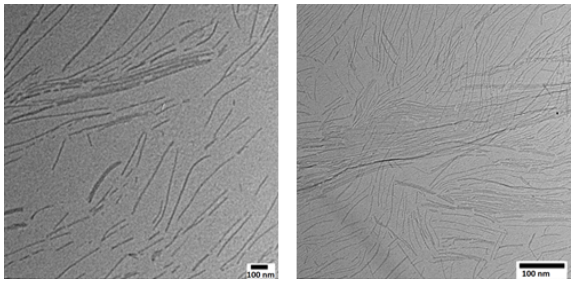

Figure 9. TEM images of polymer assembly 4 after pH 4 exposure for 2 days.

before acid triggering. This could be attributed to the conversion of the hydrophobic amine to the hydrophilic protonated ammonium salt under acidic pH, which increases the overall hydrophilic volume and thus the apparent curvature. It is interesting however that assemblies **5-6** exhibit faster release the guest molecules after pH change. This difference in the kinetics of molecular release is attributed to the accessibility of the pH-sensitive moieties in **5** and **6**, relative to **4**. This accessibility and the change in hydrophilic volume presumably cause the vesicle membrane to be more leaky for the hydrophilic guest molecules to be released from the more confined aqueous environment to the bulk. This working hypothesis is schematically represented in **Figure 10**. Overall, the studies here show that the impact of host-guest properties of a molecular assembly has to be independently evaluated, because the assembly that has the biggest influence on the morphology exhibits slow molecular release, and vice versa.

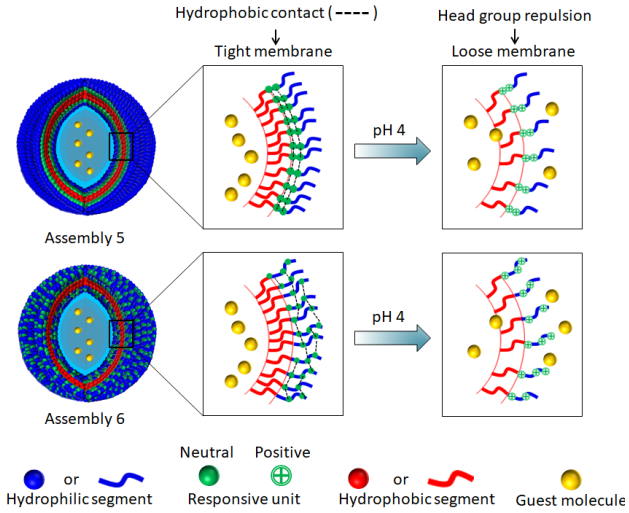

Figure 10. Schematic diagram of the purposed molecular guest release of assemblies **5** and **6.**

Conclusions

Effect of positioning pH-responsive moieties in various domains of an amphiphilic block copolymer assembly, upon its host-guest properties, has been studied. The responsive functionalities, in the form of diisopropylaminoethyl acrylate monomer, were placed in three different locations of the vesicle-forming block copolymer: (*i*) randomly distributed in the hydrophobic segment with butyl acrylate; (*ii*) incorporated as the middle block in a triblock; and (*iii*) randomly distributed in hydrophilic part of the polymer along with PEG-acrylate or hydroxyethyl-acrylate. The rate of release of guest molecules from these assemblies was indeed found to be dependent on the location of the responsive moieties. Interestingly, fastest guest release was observed with the incorporation of responsive units in hydrophilic part, while this process was the slowest when the responsive moieties are placed in the hydrophobic segment of the polymer. This observation is somewhat counter-intuitive, as it is reasonable to anticipate that the fidelity of the polymeric membrane would be compromised to a greater extent when there is a significant change in the hydrophobic domain of the membrane. Our working hypothesis here is that the accessibility of the responsive moieties to the stimulus plays a more significant role. The surprising part of this observation is due to the fact that the stimulus here is proton, arguably the smallest of the chemical stimuli. Yet another surprising observation of this work is that the most significant change in the morphology of the assembly was observed with the assembly, where the pH-responsive units are placed in the hydrophobic domain of the polymer. It is understood that the morphological change is driven by the equilibrium preference of the product polymer, while the observed molecular release variations are based on difference in kinetics. Therefore, these processes do not have to be correlated with each other. Nonetheless, an important take-home lesson here is that the ability of an assembly to release its guest molecules should not be assessed based on morphological variations alone. The importance of this finding is highlighted by the fact that many of the studies in stimulus-induced morphological changes in polymer assemblies are motivated by implications in areas such as drug delivery[16, 46]. We believe that the initial findings reported here would spur further research towards developing a deeper understanding of the reasons that underlie the host-guest properties of polymeric self-assembled nanostructures.

Conflicts of interest

There are no conflicts to declare

Acknowledgements

We thank the National Science Foundation (CHE-1745097) for funding.

Notes and references

1 J-F Lutz, *Polym. Int*. 2006, 55, 979–993.
2 C. Wang, Z. Wang, and X. Zhang, *Acc. Chem. Res*., 2012, 45, 608–618.
3 C. Lu, and M. W. Urban, *Prog. Polym. Sci*. 2018, 78, 24-46.
4 V. P. Torchilin, *Pharm. Res*. 2007, 24, 1.
5 M. C. Jones, and J. C. Leroux, *Eur. J. Pharm. Biopharm*. 1999, 48, 101-111.
6 P. Besenius, G. Portale, P. H. H. Bomans, H. M. Janssen, A. R. A. Palmans, and E. W. Meijer, *Proc. Natl. Acad. Sci. U.S.A.* 2010, 107, 17888-17893.
7 S. Bhattacharya, S. Mukherjee, J. D. Sarmab, and R. Shunmugam, *Polym. Chem*., 2018, 9, 2157-2165.
8 S. Li, J. He, M. Zhang, H. Wang, and P. Ni, *Polym. Chem*., 2016, 7, 1773-1781.
9 P. L. Soo, and A. Eisenberg, *J. Polym. Sci. Part B: Polym. Phys*. 2004, 42, 923-938.
10 C. LoPresti, H. Lomas, M. Massignani, T. Smart, and G. Battaglia, *J. Mater. Chem*., 2009, 19, 3576-3590.
11 Y. Zhu, B. Yanga, S. Chena, and J. Du, *Prog. Polym. Sci*. 2017, *64*, 1–22.
12 D. E. Discher, and A. Eisenberg, *Science* 2002, *297*, 967-973.

13 R. Erhardt, A. Boker, H. Zettl, H. Kaya, W. Pyckhout-Hintzen, G. Krausch, V. Abetz, and A. H. E. Muller, *Macromolecules* 2001, 34, 4, 1069-1075.
14 Y. Liu, C. Yu, H. Jin, B. Jiang, X. Zhu, Y. Zhou, Z. Lu, and D. A. Yan, *J. Am. Chem. Soc.*, 2013, 135, 4765–4770.
15 N. Razza, G. Rizza, P-E. Coulon, L. Didier, G. C. Fadda, B. Voit, A. Synytska, H. Grutzmacher, and M. Sangermano, *Nanoscale*, 2018, 10, 14492-14498.
16 R. T. Chacko, T. Ventura, J. Zhuang, and S. Thayumanavan, *Adv. Drug Deliv. Rev*. 2012, *64*, 836-851.
17 Q. Dai, N. Bertleff-Zieschang, J. A. Braunger, M. Björnmalm, C. Cortez-Jugo, and F. Caruso, *Adv. Healthcare Mater.* 2018, *7*, 1700575.
18 K. Dutta, D. Hu, B. Zhao, A. E. Ribbe, J. Zhuang, and S. Thayumanavan, *J. Am. Chem. Soc*. 2017, *139*, 5676−5679.
19 L. M. Randolph, C. L. M. LeGuyader, M. E. Hahn, C. M. Andolina, J. P. Patterson, R. F. Mattrey, J. E. Millstone, M. Botta, M. Scadeng, and N. C. Gianneschi, *Chemical Science*, 2016, 7, 4230–4236.
20 Q. Fan, K. Cheng, Z. Yang, R. Zhang, M. Yang, X. Hu, X. Ma, L. Bu, X. Lu, X. Xiong, W. Huang, H. Zhao, and Z. Cheng, *Adv. Mater*. 2015, *27*, 843–847.
21 L. Adamiak, J. Pendery, J. Sun, K. Iwabata, N. C. Gianneschi, and N. L. Abbott, *Macromolecules*, 2018, 51, 1978–1985.
22 P. Khomein, and S. Thayumanavan, *Chem. Commun*., 2017, *53*, 5190-5192.
23 M-K. Ng, and L. Yu, *Angew. Chem. Int. Ed.* 2002, *41*, 3598-3601.
24 M. H. Nurmawati, R. Renu, P. K. Ajikumar, S. Sindhu, F. C. Cheong, C. H. Sow, and S. Valiyaveettil, *Adv. Funct. Mater*. 2006, *16*, 2340–2345.
25 T. Terashima, T. Mes, T. F. A. De Greef, M. A. J. Gillissen, P. Besenius, A. R. A. Palmans, and E. W. Meijer, *J. Am. Chem. Soc*. 2011, *133*, 4742–4745.
26 Z. H. Farooqi, A. Ijaz, R. Begum, K. Naseem, M. Usman, M. Ajmal, and U. Saeed, *Polym. Composite*. 2016, *39*, 645-653.
27 Y. Uozumi, Y. Matsuura, T. Arakawa, and Y. M. A. Yamada, *Angew. Chem. Int. Ed*. 2009, *48*, 2708 –2710.
28 Y. Mai, and A. Eisenberg, *Chem. Soc. Rev*. 2012, *41*, 5969–5985.
29 B. Yan, X. Tong, P. Ayotte, and Y. Zhao, *Soft Matter* 2011, *7*, 10001–10009.
30 J. Du, L. Fan, and Q. Liu, *Macromolecules* 2012, *45*, 8275−8283.
31 H. Kim, Y. J. Kang, S. Kang, and K. T. Kim, *J. Am. Chem. Soc.* 2012, *134*, 4030−4033.
32 R. P. Brinkhuis, F. P. J. T. Rutjes and J. C. M. van Hest, *Polym. Chem*. 2011, *2*, 1449–1462.
33 Y-R. Kim, S. Jung, H. Ryu, Y-E. Yoo, S. M. Kim, and T-J. Jeon, *Sensors* 2012, *12*, 9530-9550.
34 M. R. Molla, P. Rangadurai, L. Antony, S. Swaminathan, J. J. de Pablo, and S. Thayumanavan, *Nat. Chem*. 2018, *10*, 659-666.
35 R. Deng, M. J. Derry, C. J. Mable, Y. Ning, S. P. Armes, *J. Am. Chem. Soc*. 2017, *139*, 7616−7623.
36 J. Zhuang, M. Garzoni, D. A. Torres, A. Poe, G. M. Pavan, and S. Thayumanavan, *Angew. Chem. Int. Ed.* 2017, *56*, 4145 –4149.
37 S. Y. Liu, J. V. M. Weaver, Y. Q. Tang, N. C. Billingham, S. P. Armes, and K. Tribe, *Macromolecules* 2002, 35, 16, 6121-6131.
38 J. Yao, Y. Ruan, T. Zhai, J. Guan, G. Tang, H. Li, and S. Dai, *Polymer* 2011, 52, 3396-3404.
39 W. Agut, A. Brulet, C. Schatz, D. Taton, and S. Lecommandoux, *Langmuir* 2010, 26, 13, 10546-10554.
40 K. E. B. Doncom, C. F. Hansell, P. Theatob, and R. K. O'Reilly, *Polym. Chem*., 2012, 3, 3007.
41 G. Kocak, C. Tuncer, and V. Bütün, *Polym. Chem*., 2017, 8, 144.
42 H. Benoit, and D. Froehlich, *Light Scattering from Polymer Solutions*; Academic Press: London, 1972.
43 C. Liu, M. A. Hillmyer, and T. P. Lodge, *Langmuir* 2009, 25, 13718–13725.
44 A. O. Moughton, and R. K. O'Reilly, *Chem. Commun*. 2010, 46, 1091–1093.
45 C. Yao, X. Wang, G. Liu, J. Hu, and S. Liu, *Macromolecules* 2016, 49, 8282−8295.
46 M. Elsabahy, and K. L. Wooley, *Chem. Soc. Rev*., 2012, 41, 2545–2561.

TOC Graphic

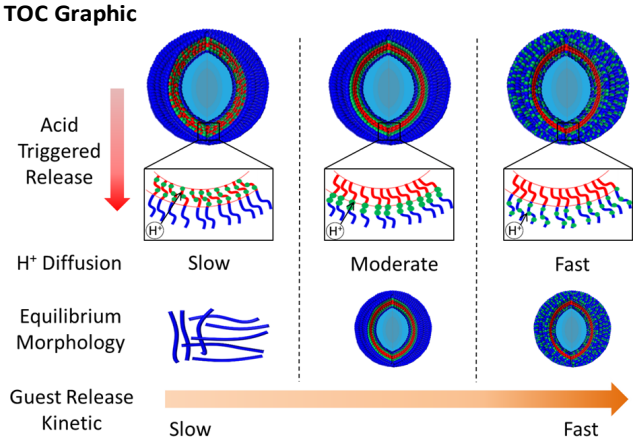
Acid
Triggered
Release
H+ Diffusion
Slow
Moderate
Fast
Equilibrium
Morphology
Guest Release
Kinetic
Slow
Fast